DOI: 10.1002/cphc.200900432

Energy Transport along Conjugated Polymer Chains with Extended Radiative Lifetimes: A Theoretical Study

Bernard Van Averbeke and David Beljonne*[a]

The ability to improve exciton diffusion lengths is a key issue in optimizing many opto-electronic devices based on conjugated polymers. On the basis of quantum-chemical calculations, we investigate a strategy consisting of extending the radiative lifetime of energy carriers through incorporation along the polymer backbone of repeating units with forbidden optical transition. The results obtained for poly(*p*-phenylenebutadiyne), PPE, and poly(*p*-triphenylenebutadiyne), PTPE, show that the larger number of hops performed by the electronic excitations during their lifetime in PTPE is compensated by the smaller hopping length (associated with the reduced conjugation length), so that similar on-chain diffusion lengths are predicted in both polymers.

1. Introduction

Resonance energy transfer (RET) is a ubiquitous photophysical process in life and materials science. Following absorption of light, the excess energy supplied to a molecule or chromophore can be dissipated by radiative decay (i.e. fluorescence or phosphorescence) as well as through monomolecular nonradiative processes (internal conversion or intersystem crossing). When several chromophores are quantum-mechanically coupled, the photoinduced electronic excitations can also undergo bimolecular events such as radiationless energy transfer.[1]

The first direct observation of electronic energy transfer was reported in photosynthetic biological antennae.[2–6] The working mechanism of light-harvesting systems designed by Nature relies on an energy gradient, resulting from a complex spatial arrangement of chromophores, which efficiently funnels the electronic excitations to the reaction center. Resonance ET plays also a crucial role in the working principle of many opto-electronic devices based on conjugated polymers, for example, in photovoltaic cells[7–12] and (bio)chemical sensors[13–26]. The charge-separation efficiency in solar cells and the detection sensitivity in sensors rely on the ability of the photoinduced electronic excitations or excitons to diffuse through the polymer organic layer toward either dissociation zones (solar cells) or recognition sites (sensors). This requires driving the electronic excitations over large distances to well-defined target sites, which is difficult to reconcile with the disordered structure inherent to most conjugated polymers.

The importance of energy diffusion in artificial light-harvesting systems has triggered intensive investigations aiming at unraveling the mechanisms ruling RET. Förster resonant energy transfer (FRET)[27], which is the most conventional approach for predicting energy transfer rates, has been recently scrutinized for its ability to account for RET in biological and nanoscale systems.[28] Gaining such a fundamental understanding is pivotal to identify strategies giving rise to efficient energy transport in synthetic light-harvesting architectures. Among such strategies, recent work has focused on improving the degree of conjugation along polymer chains through the surrounding medium[29] and on reducing the amount of energetic disorder by chemical modification of the polymer[30] as possible routes towards enhanced exciton diffusion.

An alternative approach to boost exciton diffusion lengths in conjugated polymers consists of extending the lifetime of the energy carriers. In the normal diffusion regime, the exciton mean-square displacement $\langle x^2 \rangle$ and diffusion length L_D are indeed related to the exciton lifetime τ via Equation (1)

$$L_D = \sqrt{dD\tau}, \quad D = \frac{1}{d}\lim_{t\to\infty}\frac{\langle x^2(t)\rangle}{t} \tag{1}$$

where D is the diffusion coefficient and d the dimensionality. If energy transfer follows FRET, the decrease in transition dipole moments associated with enhanced radiative lifetimes is accompanied by a decrease in diffusion coefficient, as the latter essentially involves dipole–dipole coupling. Because the two effects scale quadratically with the transition dipole moment in a weakly coupling, Förster-like picture, they should cancel out and leave L_D essentially unchanged. However, all possible mechanisms going beyond FRET could disrupt this subtle balance and have an impact on the energy-migration efficiency.

In an attempt to increase excitation transport with this approach, Swager and co-workers designed and synthesized conjugated polymers including triphenylene (TPE) units in the polymer backbone, namely, poly(triphenylenebutadiyne)s, PTPE. The triphenylene unit, which is known to have a symmetry-forbidden S_1–S_0 electronic transition, retains some of its individual characteristics in the corresponding polymers, which thereby feature increased radiative (as well as nonradiative) lifetimes in

[a] *Dr. B. Van Averbeke, Dr. D. Beljonne*
Laboratory for Chemistry of Novel Materials
University of Mons-Hainaut, Place du Parc 20, 7000 Mons (Belgium)
Fax: (+32) 65 373861
E-mail: David@averell.umh.ac.be

comparison to the reference poly(*p*-phenylenebutadiyne)s, PPE.[31] Fluorescence depolarization measurements in solution revealed higher degrees of depolarization for the TPE-based polymers, which suggest increased diffusion lengths along the PTPE polymer chains and deviations from the simple dipole–dipole mechanism.

Intrigued by these experimental results, we performed a theoretical investigation of the ground- and excited-state geometric and electronic structures of PPE and PTPE polymer chains, with the main emphasis on the interplay between conformational disorder, excited state localization, radiative lifetimes, and energy-transfer rates.

2. Theoretical Methodology

2.1. Quantum-Chemical Calculations

The optical properties of phenylenebutadiyne (OPE_n) and triphenylenebutadiyne oligomers ($OTPE_n$), where n is the number of monomer units, were computed at semiempirical and ab initio levels: INDO/SCI[32] calculations were performed on the basis of the AM1[33] (AM1/SCI) optimized ground-state (excited-state) geometries. TDDFT (TDHF) calculations were performed on the basis of the DFT-B3LYP[34,35] and PBE1PBE[36] (HF) optimized ground-state geometries. The active space used in the INDO/SCI calculations includes $20n$ molecular orbitals for OPE_n oligomers and $20n+40$ molecular orbitals for $OTPE_n$ oligomers, which is large enough to ensure full convergence of the excited-state properties (i.e., excitation energies and transition dipole moments). The radiative lifetimes in vacuum can be readily obtained by inserting the calculated transition dipole moments from the lowest excited state to the ground state μ (in debye) and the corresponding excitation frequency ν (in hertz) into the expression for the Einstein coefficient for spontaneous emission [Eq. (2)]

$$\tau_{vac}^{-1} = \frac{8\pi^2\nu^3}{3\varepsilon_0 c^3 \hbar}|\mu|^2 \quad (2)$$

Corrections due to screening and local field effects in solution were estimated by using a simple continuum dielectric model accounting for the elongated shape of the oligomers [Eq. (3)]

$$\tau^{-1} = nL^2\tau_{vac}^{-1} \quad (3)$$

where n is the refractive index of the solvent (in this case $n=$ 1.4242 for dichloromethane used in ref. [31]), and L the local field factor that relates the microscopic local electric field to the macroscopic electric field.[18] In the case of a spherical solute embedded in a solvent with the same polarizability, the field factor takes on the usual Lorentz form [Eq. (4)]

$$L_L = \frac{n^2+2}{3} \quad (4)$$

For elongated (ellipsoidal) molecules and different (isotropic) polarizabilities between solute and solvent, L is written as Equation (5)

$$L = \frac{n^2}{n^2 + (1-n^2)A_c - 3A_c(a-A_c)(n^2-1)\frac{\chi}{4\pi\varepsilon_0 abc}} \quad (5)$$

where A_c is a geometrical factor related to the cylindrical shape of the molecule[37], a, b, and c are the principal axes of the ellipsoidal cavity representing the solute, and χ is the polarizability of the molecule, calculated here at the AM1 level.[33]

2.2. Electronic Coupling and Energy-Transfer Rates

To disentangle the long-range (Coulombic or "through-space", TS) and direct overlap ("through-bond", TB) contributions to the electronic coupling between conjugated segments along the same polymer chain (see ref. [38] for more details), we calculated the excited-state splitting in symmetric bichromophoric configurations defined by introducing a torsion angle ϕ (ranging from 0 to 90°) between the two innermost units. For $\phi=90°$, the wavefunction overlap between the donor and acceptor subunits is zero, so that only TS contributions are operative. At smaller angles, both TB and TS interactions contribute to the overall splitting. We also computed directly the Coulomb excitonic couplings entering a Förster-like model for RET. To account for the detailed chemical structures of the interacting conformational subunits, a multipolar representation of the transition dipole moments was used. Within this distributed monopole model, the electronic couplings are expressed as a sum over pairwise interactions between INDO/SCI atomic transition densities associated with the relevant excited states of the interacting chromophores [Eq. (6)][39–44]:

$$V_{da} = \frac{1}{4\pi\varepsilon_0}\sum_m\sum_n q_d(m)q_a(n)V(m,n) \quad (6)$$

where $q_d(m)$ [$q_a(n)$] represents the transition density on site m [n] for the lowest optical excitation of the donor [acceptor], and $V(m,n)$ the electron–electron interaction potential, here taken to be the Mataga–Nishimoto potential as implemented in ZINDO.[45] Note that gas phase transition densities were used here, as we expect the nearest-neighbor interactions that are primarily involved in the energy-diffusion process to be only weakly affected by the local environment.[46]

Assuming weak couplings between molecules, the energy transfer rate from donor to acceptor is given by the Fermi golden rule [Eq. (7)]

$$k_{da} = \frac{2\pi}{\hbar}|V_{da}|^2 J_{da} \quad (7)$$

where J_{da} represents the spectral overlap between the donor emission and the acceptor absorption spectra, normalized on an energy scale. The optical spectra were simulated by using an undistorted, displaced, harmonic-oscillator model accounting for two effective vibrational modes: 1) a "high-frequency" mode, representative of the dominant carbon–carbon stretching and ring-breathing vibrational motions; and 2) a "low-fre-

quency" mode, that accounts for the librational motions between repeating units but also effectively encompasses modes associated with the solvent bath.[47–49]

The Huang–Rhys factors S_i associated with each vibrational mode with frequency ν_i, are extracted from the corresponding relaxation energies E_i^{rel} by using Equation (8)

$$S_i = \frac{E_i^{rel}}{h\nu_i} \quad (8)$$

These factors provide a direct measurement of the changes in equilibrium geometry along normal mode *i* on going from the ground-state to the lowest electronic excited-state equilibrium geometry. In this work, the energy of the high-frequency modes is fixed to a value of 0.2 eV, and we extract the corresponding S_i factors from the relaxation energies calculated at the AM1/SCI level for planar conformers. The frequency and displacements for the low-frequency mode are adjusted to reproduce the Stokes shifts measured for PTPE and PPE in methylene chloride (ca. 0.24 and ca. 0.15 eV, respectively).[31]

3. Results and Discussion

3.1. Equilibrium Ground-State Geometries

Spectroscopic properties of conjugated polymers and molecules strongly depend on their geometric structure. We thus explored the configurational space of several OPE_n and $OTPE_n$ oligomers at different levels of theory (AM1, HF, and DFT). More specifically, we focused on two geometrical parameters that directly determine the overall conformation and rigidity of the polymer chains, namely, the dihedral angle ϕ between successive repeating units and the bond angle θ around a triple bond, respectively (see Scheme 1).

At all levels of theory, we found two local minima for $\phi \approx 0$–25° and 180° in both series of oligomers, corresponding to *syn* and *anti* configurations of the bulky triphenylene units in $OTPE_n$ (see Scheme 1). As expected from the cylindrical symmetry of the triple bonds, the potential-energy surface along the interunit dihedral angle is very flat in oligophenylenebutadiynes, with a barrier height at 90° on the order of *kT* at room temperature. The barrier is larger in oligotriphenylenebutadiynes because of the steric hindrance generated by the bulky triphenylene units.

Table 1 collects the ground-state energies of some relevant geometric configurations for a model dimer. Most strikingly, the equilibrium bond angle in $OTPE_2$ significantly shifts from the ideal linear configuration, with $\theta_{eq} \approx 175^\circ$ at both AM1 and DFT levels (the corresponding angle is 180° in OPE_2). This deviation from the geometric structure expected for sp-hybridized carbon atoms originates from the steric hindrance between the triple bond and the triphenylene moiety and results in bent structures, as shown in Scheme 2.

The calculated equilibrium geometries provide an alternative framework to rationalize the increased depolarization measured by Swager and co-workers in PTPE.[31] One would indeed expect faster depolarization of the photoluminescence signal

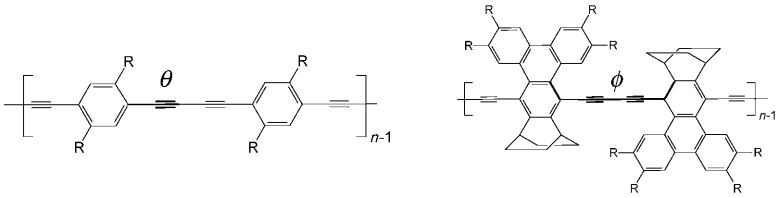

Scheme 1. Chemical structures and relevant bond angle θ and dihedral angle ϕ in OPE_n and $OTPE_n$ oligomers. R = OCH_3.

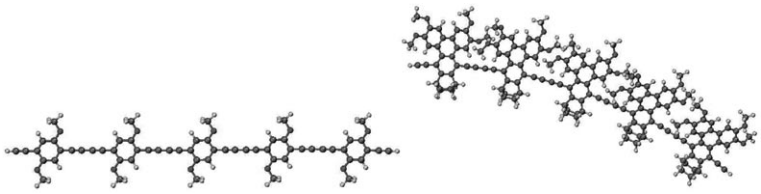

Scheme 2. Rigid and bent structures of OPE_4 and $OTPE_4$, respectively.

Table 1. Relative energies for different geometric configurations of OPE_2 and $OTPE_2$ dimers.

	Dihedral angle (ϕ)				Bond angle (θ)			
	DFT-B3LYP		HF		AM1		DFT-B3LYP	
	ϕ [°]	E_{rel} [kcal mol^{-1}]	ϕ [°]	E_{rel} [kcal mol^{-1}]	θ [°]	E_{rel} [kcal mol^{-1}]	θ [°]	E_{rel} [kcal mol^{-1}]
	20.4	0	25.3	0	170	0.4	170	2.03
$OTPE_2$	90[a]	1.77	90	1.15[a]	175	0	175	0
	179.7	1.07	175.6	0.49	180	0.17	180	0.7
	0	0	0	0	170	1	170	6
OPE_2	90[a]	0.53	90	0.3[a]	175	0.21	175	1.8
	179.9	0.17	179.9	0.2	180	0	180	0

[a] Transition state.

in chains that are prone to adopting a banana shape, as is the case for PTPE as opposed to the stiffer PPE. We applied a random growth algorithm to generate PTPE and PPE polymer chains based on the B3LYP bond-angle potential. Examples of chains that we obtained with this approach are shown in Figure 1: the PTPE chains adopt a coiled-like arrangement as opposed to the rigid-rod PPE chains. This is quantified by the calculated end-to-end distances of $\langle R_{ee} = 92$ nm in PPE and

Figure 1. OPE_{100} (left) and $OTPE_{100}$ chains (right) generated from a random-growth algorithm based on the B3LYP potential for the bond angle θ.

$\langle R_{ee} \rangle = 42$ nm in PTPE, after averaging over 1000 realizations of a 100-unit-long polymer chain. Our simulations for PPE qualitatively reproduce the trends observed experimentally by Swager et al. that low molecular weight fractions of this polymer show rigid-rod behavior[50]. On the other hand, PTPE chains show a higher propensity to behave as "wormlike" chains.

3.2. Electronic Coupling

In this section, we discuss electronic coupling in OPE_n and $OTPE_n$ oligomers, considering both through-space and through-bond contributions and focusing mainly on the influence of units with long radiative lifetime along the polymer backbone. As in ref. [38], we consider a symmetric "donor (D)–acceptor (A)" bichromophore (where D≡A) with the two planar conjugated segments separated by a conformational kink (the dihedral angle ϕ between the innermost repeating units). The total coupling is then obtained as half the energy splitting between the lowest two adiabatic excited states of the system. The results obtained for $OTPE_n$ and OPE_n of equivalent sizes are reported in Figure 2.

As reported previously in the case of OPE_n-based bichromophores,[38] a strong decrease in electronic coupling is calculated 1) with increasing dihedral angle as a result of the reduced overlap between the donor and acceptor wavefunctions and the resulting lower TB contributions, and 2) with increasing conjugation length, because of the reduced end-to-end overlap in the more extended π-conjugated segments (smaller TB contributions) together with the larger center-to-center separation (smaller TS contributions).

Figure 2 also shows that the electronic couplings (both TB and TS) are smaller in $OTPE_n$ than in OPE_n of similar lengths. This can be understood from the "crossed π delocalization" over the repeating TPE units, which reduces the weights of the wavefunction along the polymer chains and therefore also the

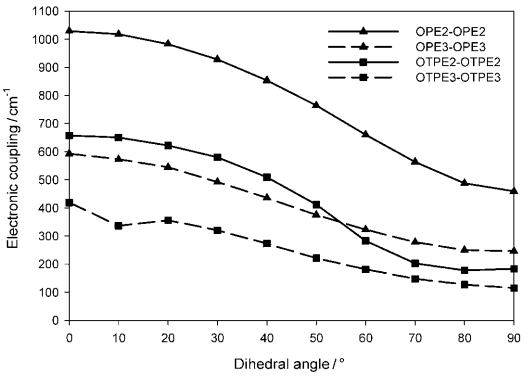

Figure 2. Evolution of the total electronic coupling with dihedral angle between the two innermost units of OPE_n/$OTPE_n$-based bichromophores.

"longitudinal" delocalization. As a result, triphenylene-based polymer chains should be more prone to disorder-induced excited-state localization. In addition, as the quantum-chemical interactions mediating energy diffusion are weaker, less efficient energy transport is expected along TPE-based polymers, whatever the actual mechanism (TS vs TB, weak vs strong coupling).

3.3. Spectroscopic Properties

The INDO/SCI vertical excitation energies computed for molecules in their electronic ground-state and excited-state geometric structures and the corresponding radiative lifetimes (in the gas phase and corrected for solvent-screening effects) are presented in Table 2.

From Table 2, the following conclusions can be drawn: 1) A systematic lowering of the lowest optical transition energy is predicted at all levels of theory on going from OPE_n to $OTPE_n$, in good agreement with experiment, and the energy difference decreases with increasing oligomer length. For instance, the INDO/SCI vertical transition energy from the ground-state geometry is about 0.6 eV smaller in $OTPE_1$ than in OPE_1, while the corresponding energy difference is only about 0.1 eV for the hexamers ($n = 6$). This points to different dependences of the spectroscopic properties on the number of repeating units in the two different polymers. 2) There are significant quantitative differences between the excitation energies computed by the different approaches. While TDHF strongly overestimates the vertical transition energies in all cases, the TDDFT calculations yield results that are similar to INDO/SCI for short chains but significantly lower values in extended π systems. This can be traced back to issues related to a proper description of long-range interactions with the common DFT functionals.[34,51–56]

It is also instructive to plot the chain-length-dependent bathochromic shift with respect to monomer absorption, as this provides direct insight into the degree of electronic communication along the conjugated chains. The results, reported in Figure 3 and fully supported by the experimental spectroscopic data, show that the overall energy stabilization from monomer to polymer is about two times smaller in PTPE compared to PPE. In addition, the excitation energies converge

Table 2. Calculated vertical excitation energies for absorption E_{abs} and emission E_{emn} in OPE_n/$OTPE_n$ as a function of oligomer length.

	n	E_{abs} (INDO/SCI) [eV]	E_{emn} (INDO/SCI) [eV]	E_{abs} (TDDFT-B3LYP) [eV]	E_{abs} (TDDFT-PBE1PBE) [eV]	E_{abs} (TDHF) [eV]
OPE_n	1	3.91	3.82	3.87	3.95	4.84
	2	3.18	2.82	2.94	3.03	4.11
	3	3.04	2.78	2.55	2.65	3.88
	4	2.97	2.73	2.35	2.46	3.78
	5	2.93	2.73	–	–	–
	6	2.91	2.73	–	–	–
	7	2.89	2.73	–	–	–
	PPE (exptl)[a]	E_{abs} = 2.88 eV, E_{emn} = 2.73 eV				
$OTPE_n$	1	3.35	3.13	3.2	3.34	4.34
	2	2.97	2.64	2.57	2.69	3.91
	3	2.88	2.67	2.29	2.4	3.73
	4	2.84	2.57	–	–	–
	5	2.82	2.57	–	–	–
	6	2.82	2.57	–	–	–
	TPPE (exptl)[b]	E_{abs} = 2.58 eV, E_{emn} = 2.34 eV				

[a] Poly(1,4-diethynyl-6-methoxy-3-decyloxybenzene) in dichloromethane.[31] [b] Poly[2,3-(1,4-cyclohexanylene)-1,4-diethynyl-6,7,10,11-tetraethylhexyloxytriphenylene] in dichloromethane.[31]

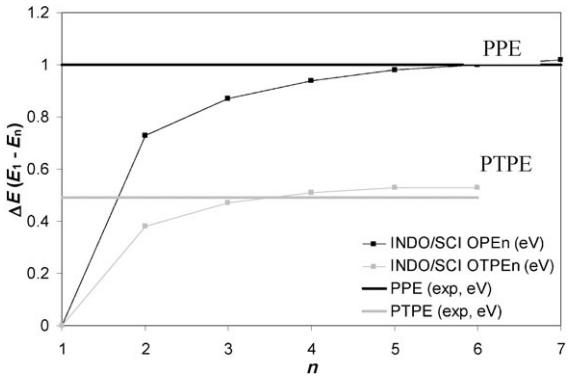

Figure 3. Chain-length-dependent INDO/SCI bathochromic displacements from monomer to *n*-mer in OPE_n and $OTPE_n$. The measured shifts between the monomer and polymer absorption peaks in methylene chloride solutions are shown for comparison.[57]

faster to their asymptotic values in PTPE (after about three repeating units in $OTPE_n$ as opposed to about six in OPE_n). These two findings support the view presented above that electronic coupling between the repeating units is significantly smaller in the triphenylene-based polymer.

The radiative lifetimes inferred from semiempirical and ab initio quantum-chemical excited-state calculations are reported in Table 3, which shows that: 1) Both semiempirical and ab initio quantum-chemical calculations reproduce qualitatively the measured enhanced radiative lifetimes from OPE_n to $OTPE_n$. Inclusion of implicit solvent results in lower radiative lifetimes, as expected from screening effects. 2) Except for the monomer and the TDHF results, all methods provide consistent radiative lifetimes in OPE_n. 3) The $OTPE_n$ oligomers with $n \geq 2$ display radiative lifetimes that are significantly smaller than that of the monomer (>100 ns[31]), indicative of at least

Table 3. Computed radiative lifetimes τ_R for OPE_n and $OTPE_n$ oligomers.

Polymer	n	τ_R (INDO/SCI, vacuum) [ns]	τ_R (INDO/SCI, CH_2Cl_2) [ns]	τ_R (DFT-B3LYP, vacuum) [ns]	τ_R (DFT-PBE1PBE, vacuum) [ns]	τ_R (HF, vacuum) [ns]
OPE_n	2	4.25	2.6	1.89	1.78	1.06
	3	1.99	1.28	1.39	1.24	0.65
	4	1.48	0.98	1.09	1.01	0.47
	5	1.16	0.78	–	–	–
	6	0.98	0.67	–	–	–
	7	0.86	0.59	–	–	–
	PPE (exptl)[a]	0.9				
$OTPE_n$	2	5.69	3.08	5.19	4.43	1.99
	3	2.63	1.57	2.67	2.45	1.04
	4	2.18	1.54	1.99	1.85	–
	5	2.44	1.4	–	–	–
	6	1.7	1.12	–	–	–
	PTPE (exptl)[b,c]	6.7,[b] 9[c]				

[a] Poly(1,4-diethynyl-6-methoxy-3-decyloxybenzene) in dichloromethane.[31] [b] Poly[2,3-[1,4-cyclohexanylene]-1,4-diethynyl-6,7,10,11-tetraethylhexyloxy-triphenylene] in dichloromethane.[31] [c] Poly(1,4-diethynyl-6,7,10,11-tetraethylhexyloxytriphenylene) in dichloromethane.[57]

some conjugation disturbing the threefold symmetry of the triphenylene moieties. In the case of OPE_n, theory and experiment shows a reasonable agreement when the measured radiative lifetimes are compared to those calculated for the longest conjugated segments (5–7 repeating units). In contrast, the calculations suggest that a much smaller radiative lifetime would be obtained regardless of the methodology used if the effective conjugation length in $OTPE_n$ exceeded two monomer units. In view of the overall reasonable agreement between the measured and calculated spectroscopic data and the fact that the same trends are observed irrespective of the applied quantum-chemical approach, we conclude that the conjugation length in PTPE must be significantly shorter than in PPE. This is fully consistent with the electronic coupling analysis above and suggests that conformational disorder chops off the polymer chains into subsegments that are on average 5–7 repeating units long in PPE but only 2–3 units long in PTPE.

Table 4. Energy-hopping parameters for different combinations of donors and acceptors.

OPE_n					$OTPE_n$				
n_D	n_A	V_{DA} [cm^{-1}]	J_{DA} [cm]	k_{DA} [ps^{-1}]	n_D	n_A	V_{DA} [cm^{-1}]	J_{DA} [cm]	k_{DA} [ps^{-1}]
2	2	183	1.23×10^{-5}	0.49	2	2	120	2.41×10^{-5}	0.41
	3	161	7.85×10^{-5}	2.41		3	115	6.04×10^{-5}	0.94
	4	133	1.21×10^{-4}	2.54		4	95	8.88×10^{-5}	0.94
	5	111	1.54×10^{-4}	2.22		5	64	1.03×10^{-4}	0.49
	6	94	1.7×10^{-4}	1.77		6	–	–	–
	7	80	1.78×10^{-4}	1.35		7	–	–	–
3	3	145	4.92×10^{-5}	1.23	3	3	107	3.44×10^{-5}	0.46
	4	123	8.98×10^{-5}	1.6		4	90	6.04×10^{-5}	0.57
	5	104	1.12×10^{-4}	1.42		5	62	7.18×10^{-5}	0.32
	6	88	1.25×10^{-4}	1.14		6	–	–	–
	7	77	1.33×10^{-4}	0.92		7	–	–	–
4	4	96	3.81×10^{-5}	0.41	4	4	64	3.11×10^{-5}	0.15
	5	82	5.4×10^{-5}	0.43		5	46	3.8×10^{-5}	0.09
	6	70	7.16×10^{-5}	0.42		6	–	–	–
	7	62	7.91×10^{-5}	0.36		7	–	–	–

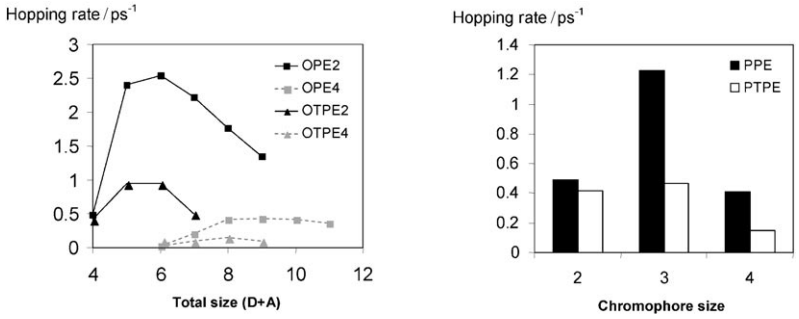

Figure 4. Energy transfer rates as a function of acceptor size for donor sizes $N_D=2$ and $N_D=4$ (left) and for $N_D=N_A$ (right).

3.4. Energy-Transfer Rates

We now turn to the energy-transfer rates, as computed in the weak coupling regime and retaining only the through-space contributions to the electronic coupling. We previously showed that conformational subunits along PPE chains interact mostly by weak Coulombic coupling.[38] The electronic couplings and spectral overlaps between different combinations of donors and acceptors of increasing size are listed in Table 4.

Table 4 shows that 1) $V_{DA}(OPE_n) > V_{DA}(OTPE_n)$. This result has been discussed previously and originates from the reduced transition dipoles of the long-radiative-lifetime $OTPE_n$ oligomers compared to OPE_n oligomers of the same length. 2) The electronic coupling diminishes with increasing donor and acceptor size owing to the increased center-to-center separation. 3) Because the spectral overlaps are similar in both types of oligomers, OPE_n exhibit larger hopping rates than $OTPE_n$ of equivalent lengths. This is illustrated in Figure 4, which shows the nearest-neighbor hopping rates for donors and acceptors of different sizes.

Thus, despite the fact that electronic excitations on PTPE polymer chains have longer (radiative) lifetimes, their diffusion is slower. The two effects may therefore cancel out to yield similar exciton diffusion lengths in dilute solutions of both polymers. The quantitative determination of exciton diffusion lengths is beyond the scope of this work, as it critically depends on the conformational potential-energy surface of the polymers, which itself varies with the nature of the solvent, side chains, temperature, and so on.

A rough estimate of L_D can be obtained from a random-walk model and by use of Equation (1) with averaged hopping rates and hopping distances calculated between conjugated segments of about 2–3 repeating units in PTPE and about 5–7 units in PPE (corresponding to the averaged conjugation lengths inferred for both polymers from the spectroscopic results).

The averaged hopping rates calculated for short $OTPE_n$ and long OPE_n oligomers are very similar, but the distance covered by a single hopping step (l_{hop} in Table 5) is 1.5–3 times larger in PPE chains with extended conjugation, and the exciton lifetime 3–6 times smaller. Altogether, this results in diffusion lengths that are of comparable magnitudes when taking into account the large uncertainties in the model. Note that these values are very likely largely overestimated, as energetic and positional disorders have been neglected. More work is therefore needed to rationalize the larger depolarization of the photoluminescence measured in triphenylene-based polymers

Table 5. L_D values in PPE and PTPE chains obtained from a random-walk model and by assuming different conjugation lengths n_{conj}; l_{hop} is the hopping distance taken to the center-to-center separation.

	n_{conj}	k_{DA} [ps^{-1}]	l_{hop} [nm]	τ_R [ps]	L_D [nm]
	2	0.31	1.87	5690	79
TPPE	3	0.37	2.8	2670	88
	4	0.17	3.7	2180	71
	5	0.45	4.98	1160	114
PPE	6	0.29	5.64	980	95
	7	0.13	6.86	860	73

compared to PPE and previously ascribed to improved exciton diffusion along polymer chains incorporating extended-lifetime units.[31] Though definitive conclusions cannot be drawn at this stage, it is useful to recall that PTPE chains very likely display shorter persistence lengths than their PPE counterparts, as a result of steric hindrance induced by the bulky triphenylene groups. For similar diffusion lengths to those predicted here, PTPE would thus show enhanced emission depolarization.

4. Conclusions

We have assessed the spectroscopic features of triphenylene-based polymer chains using both semi-empirical and ab initio theoretical approaches. The detailed analysis of the ground-state equilibrium geometries revealed that PTPE shows bent, banana-like structures owing to steric effects associated with the bulky side groups. The calculated radiative lifetimes for oligomers of increasing length show good agreement with the experimental results in the corresponding polymers, if one assumes a smaller effective conjugation length in PTPE compared to PPE. This is fully consistent with the reduced electronic coupling between the repeating units along the PTPE chains. In the weak-coupling regime, similar hopping rates are computed between subunits of the averaged conjugation lengths in both polymer chains. On that basis, the increased lifetime should result in a larger exciton diffusion length in PTPE. A simple random-walk model, however, yields comparable L_D values, as the larger number of hops performed by a singlet excitation within its lifetime in PTPE is compensated by the smaller hopping distance (associated with the reduced conjugation length). The increased depolarization observed experimentally for PTPE and other polymers with enhanced radiative lifetimes is therefore not supported by the hopping calculations presented here. We are now extending these calculations to the strong-coupling regime to check whether the same conclusions would apply in this case. Alternatively, the bent equilibrium conformation of PTPE chains might play a central role in depolarizing light emission as excitons migrate along the polymer chains.

Acknowledgements

This work is supported by the Interuniversity Attraction Pole program of the Belgian Federal Government (PAI 6/27), the European Commission via Project MODECOM (NMP-CT-2006-016434), and the Belgian National Fund for Scientific Research (FNRS). D.B. is a FNRS research director. B.V.A. acknowledges a grant from FRIA (Fonds pour la formation à la Recherche dans l'Industrie et dans l'Agriculture). We thank Prof. T. Swager for stimulating discussions and for sending us the PhD thesis of A. Rose.

Keywords: ab initio calculations · conjugation · energy transfer · excitons · polymers

[1] B. W. Van Der Meer, G. Coker, S.-Y. S. Chen, *Resonance Energy Transfer: Theory and Data*, VHC, New York, **1994**.
[2] R. Van Grondelle, J. P. Dekker, T. Gillbro, V. Sundström, *Biochem. Biophys. Acta* **1994**, *1187*, 1.
[3] V. Sundström, T. Pullerits, R. Van Grondelle, *J. Phys. Chem. B* **1999**, *103*, 2327.
[4] G. D. Scholes, G. R. Fleming, *J. Phys. Chem. B* **2000**, *104*, 1854.
[5] A. P. Schreve, J. K. Trautman, H. A. Franck, T. G. Owens, A. C. Albrecht, *Biochem. Biophys. Acta* **1991**, *1058*, 280.
[6] R. Jimenez, S. N. Dikshit, S. E. Bradforth, G. R. Fleming, *J. Phys. Chem.* **1996**, *100*, 6825.
[7] J. J. M. Halls, C. A. Walsh, N. C. Greenham, E. A. Marseglia, R. H. Friend, S. C. Moratti, A. B. Holmes, *Nature* **1995**, *376*, 498.
[8] N. S. Sariciftci, L. Smilowitz, A. J. Heeger, F. Wudl, *Science* **1992**, *258*, 1474.
[9] M. Theander, A. Yartsev, D. Zigmantas, V. Sundstrom, W. Mammo, M. R. Andersson, O. Inganas, *Phys. Rev. B* **2000**, *61*, 12957.
[10] J. J. M. Halls, K. Pichler, R. H. Friend, S. C. Moratti, A. B. Holmes, *Appl. Phys. Lett.* **1996**, *68*, 3120.
[11] H. Hoppe, M. Niggemann, C. Winder, J. Kraut, R. Hiegsgen, A. Hinsch, D. Meissner, N. S. Saricifti, *Adv. Func. Mater.* **2004**, *14*, 1005.
[12] S. Günes, H. Neugebauer, N. S. Sariciftci, *Chem. Rev.* **2007**, *107*, 1324.
[13] K. P. R. Nilsson, O. Inganäs, *Macromolecules* **2004**, *37*, 9109.
[14] K. P. R. Nilsson, J. D. M. Olsson, P. Konradsson, O. Inganäs, *Macromolecules* **2004**, *37*, 6316.
[15] P. Björk, N.-K. Persson, K. P. R. Nilsson, P. Åsberg, O. Inganäs, *Biosens. Bioelectron.* **2005**, *20*, 1764.
[16] K. P. R. Nilsson, J. Rydberg, L. Baltzer, O. Inganäs, *Proc. Natl. Acad. Sci. USA* **2004**, *101*, 11197.
[17] Q. Zhou, T. M. Swager, *J. Am. Chem. Soc.* **1995**, *117*, 12593.
[18] S. W. Thomas III, G. D. Joly, T. M. Swager, *Chem. Rev.* **2007**, *107*, 1339.
[19] D. T. McQuade, A. H. Hegedus, T. M. Swager, *J. Am. Chem. Soc.* **2000**, *122*, 12389.
[20] L. Chen, D. W. McBranch, H.-L. Wang, R. Helgeson, F. Wudl, D. G. Whitten, *Proc. Natl. Acad. Sci. USA* **1999**, ***96***, 12287.
[21] D. Wang, X. Gong, P. S. Heeger, F. Rinisland, G. C. Bazan, A. J. Heeger, *Proc. Natl. Acad. Sci. USA* **2002**, *99*, 49.
[22] X. Gong, S. Wang, D. Moses, G. C. Bazan, A. J. Heeger, *Adv. Funct. Mater.* **2005**, *17*, 2053.
[23] M. Stork, B. S. Gaylord, A. J. Heeger, G. C. Bazan, *Adv. Mater.* **2002**, *14*, 361.
[24] S. J. Dwight, B. S. Gaylord, J. W. Hong, G. C. Bazan, *J. Am. Chem. Soc.* **2004**, *126*, 16850.
[25] K. Doré, S. Dubus, H.-A. Ho, I. Levesque, M. Brunette, G. Corbeil, M. Boissinot, G. Boivin, M. G. Bergeron, D. Boudreau, M. Leclerc, *J. Am. Chem. Soc.* **2004**, *126*, 4240.
[26] H.-A. Ho, A. Najari, M. Leclerc, *Acc. Chem. Res.* **2008**, *41*, 168.
[27] Th. Förster, *Ann. Phys.* **1948**, *2*, 45.
[28] D. Beljonne, C. Curutchet, G. D. Scholes, R. J. Silbey, *J. Phys. Chem. B* **2009**, *113*, 6583.
[29] E. E. Nesterov, Z. Zhu, T. M. Swager, *J. Am. Chem. Soc.* **2005**, *127*, 10083.
[30] D. E. Markov, C. Tanase, P. W. M. Blom, J. Wildeman, *Phys. Rev. B* **2005**, *72*, 045217.
[31] A. Rose, C. G. Lugmair, T. M. Swager, *J. Am. Chem. Soc.* **2001**, *123*, 11298.
[32] J. Ridley, M. C. Zerner, *Theor. Chim. Acta* **1973**, *32*, 111.
[33] M. J. S. Dewar, E. G. Zoebisch, E. H. Healy, J. J. P. Stewart, *J. Am. Chem. Soc.* **1985**, *107*, 3902; AMPAC 8, **1992**–**2004**, Semichem, Inc. PO Box 1649, Shawnee, KS 66222.

[34] A. D. Becke, *J. Chem. Phys.* **1993**, *98*, 5648.
[35] C. Lee, W. Yang, R. G. Parr, *Phys. Rev. B* **1988**, *37*, 785.
[36] J. P. Perdew, K. Burke, M. Ernzerhof, *Phys. Rev. Lett.* **1996**, *77*, 3865.
[37] R. A. L. Vallée, M. Van Der Auweraer, F. C. De Schryver, D. Beljonne, M. Orrit, *ChemPhysChem* **2005**, *6*, 81.
[38] B. Van Averbeke, D. Beljonne, E. Hennebicq, *Adv. Funct. Mater.* **2008**, *18*, 492.
[39] D. Beljonne, J. Cornil, R. Silbey, P. Millié, J. L. Brédas, *J. Chem. Phys.* **2000**, *112*, 4749.
[40] K. F. Wong, B. Bagchi, P. J. Rossky, *J. Phys. Chem. A* **2004**, *108*, 5752.
[41] W. Barford, *J. Chem. Phys.* **2007**, *126*, 134905.
[42] G. D. Scholes, G. D. Fleming, *J. Phys. Chem. B* **2000**, *104*, 1854.
[43] E. Hennebicq, G. Pourtois, G. D. Scholes, L. M. Herz, D. M. Russell, C. Silva, S. Setayesh, A. C. Grimsdale, K. Mullen, J. L. Brédas, D. Beljonne, *J. Am. Chem. Soc.* **2005**, *127*, 4744.
[44] S. Westenhoff, A. Abrusci, W. J. Feast, O. Henze, A. F. M. Kilbinger, A. P. H. J. Schenning, C. Silva, *Adv. Mater.* **2006**, *18*, 1281.
[45] N. Mataga, K. Nishimoto, *Z. Phys. Chem.* **1957**, *13*, 140.
[46] G. D. Scholes, C. Curutchet, B. Mennucci, R. Cammi, J. Tomasi, *J. Phys. Chem. B* **2007**, *111*, 6978.
[47] B. Van Averbeke, D. Beljonne, *J. Phys. Chem. A* **2009**, *113*, 2677.
[48] S. Athanasopoulos, E. Hennebicq, D. Beljonne, A. B. Walker, *J. Phys. Chem. C* **2008**, *112*, 11532.
[49] T. E. Dykstra, E. Hennebicq, D. Beljonne, J. Gierschner, G. Claudio, E. R. Bittner, J. Knoester, G. D. Scholes, *J. Phys. Chem. B* **2009**, *113*, 656.
[50] P. M. Cotts, T. M. Swager, Q. Zhou, *Macromolecules* **1996**, *29*, 7323.
[51] P. J. Stephens, J. F. Devlin, C. F. Chabalowski, M. J. Frisch, *J. Chem. Phys.* **1993**, *98*, 11 623.
[52] R. Bauernschmitt, R. Ahlrichs, *Chem. Phys. Lett.* **1996**, 256, 454.
[53] D. J. Tozer, N. C. Handy, *J. Chem. Phys.* **1998**, *109*, 10180.
[54] D. J. Tozer, R. D. Amos, N. C. Handy, B. O. Roos, L. Serrano-Andres, *Mol. Phys.* **1999**, *97*, 859.
[55] A. Dreuw, J. L. Weisman, M. Head-Gordon, *J. Chem. Phys.* **2003**, *119*, 2943.
[56] L. Bernasconi, M. Sprik, J. Hutter, *J. Chem. Phys.* **2003**, *119*, 12417.
[57] A. Rose, *Optimizing the Excited State Processes of Conjugated Polymers for Improved Sensory Response*, Ph. D. Thesis, MIT, **2003**.

Received: June 4, 2009
Published online on October 20, 2009

